

Construction and Application of Experimental Platform for Measuring Resistance Coefficient of Micro-nanoporous Membrane

Anding Yang^a, Dianzheng Zhuang^b

Shenyang University of Technology, Shenyang 110000, China

^aandingy@smail.sut.edu.cn, ^bzhuangdianzheng@sut.edu.cn

Abstract

To accurately measure the viscous and inertial resistance coefficients of micro/nanoporous membranes, an experimental platform was designed and constructed to characterize their resistance properties. The experiment involved measuring pressure drop variations at different flow velocities and fitting their relationship to precisely determine the viscous resistance coefficient. To ensure the reliability of the experimental data, computational fluid dynamics (CFD) simulations were performed to conduct a numerical analysis of the experimental results. A comparison between the simulation and experimental data confirmed the feasibility and effectiveness of the proposed measurement method. The findings of this study have broad applications in fields such as gas diffusion, electrodialysis, and filtration-separation, providing valuable insights for enhancing the practical performance of micro/nanoporous membranes.

Keywords

Micro/Nanoporous Membrane; Resistance Coefficient; CFD Simulation.

1. Introduction

In recent years, with the in-depth research on micro/nanoporous membranes by scientists, they have demonstrated significant application potential in various fields, including biomedical and water treatment applications^[1-3]. Despite numerous studies exploring the performance of micro/nanoporous membranes across different industries, research on the physical properties of microporous membranes remains limited. Guozhong Wu et al^[4] developed a resistance coefficient measurement device based on porous medium oil-water migration, studying the flow resistance characteristics of water and oil as working fluids and fitting the velocity-pressure drop curve to calculate the viscous and inertial resistance coefficients. Li Xin et al^[5] invented a method that uses sensors to measure the pressure drop and flow velocity before and after fluid flows through porous materials, allowing for the calculation of the resistance coefficient by fitting the velocity-pressure drop equation. This method offers high calculation accuracy. In this study, we also employ this approach to measure the resistance coefficients of foam titanium membranes and ceramic membranes.

2. Experimental Theory and Equipment

In oxygenated aeration reaction systems, the mass transfer efficiency at the gas-liquid interface is significantly influenced by the bubble size distribution and dynamic behavior, which in turn determines the reaction kinetics and product generation efficiency. Due to their uniform micropore distribution characteristics, porous ceramic membranes and foam titanium membranes have become ideal carriers for the efficient generation of micro/nanobubbles. The mechanism of action lies in the

fact that pressurized gas, passing through the membrane pores, undergoes shear effects, forming submillimeter to micro/nanometer-sized bubbles. This process optimizes mass transfer by increasing the specific surface area and interface renewal rate.

The viscous resistance coefficient (Darcy resistance coefficient) was first introduced by the French engineer Henry Darcy in 1856^[6]. Darcy discovered the law governing fluid flow through porous media while conducting experiments on water flow in sand layers. This discovery became a fundamental basis for describing flow resistance. He established the basic principles of flow through porous media, providing important theoretical support for subsequent research. The inertial resistance coefficient (Forchheimer resistance coefficient) was first proposed by the German engineer Franz von Forchheimer in 1901^[7]. The inertial resistance coefficient is used to modify Darcy's law to account for nonlinear effects and the impact of turbulence on flow resistance. This coefficient considers the effect of fluid turbulence on flow resistance, allowing the model to more accurately describe flow behavior.

2.1 Micro/Nanoporous Membrane Sample Parameters

The micro/nanoporous membrane samples used in this experiment are silicon carbide foam ceramic membranes (hereinafter referred to as ceramic membranes) and foam titanium membranes (hereinafter referred to as titanium membranes). The silicon carbide foam ceramic membrane is a porous material with high stability, corrosion resistance, and good chemical stability, and has been widely applied in filtration, catalysis, and other fields. The titanium membrane is a porous material with a high specific surface area, excellent mechanical properties, and outstanding corrosion resistance, and is commonly used in catalyst support, filtration, and bone replacement materials. The basic parameters of the membranes used in the experiment are shown in Table 1.

Table 1. Basic Parameters of Micro/Nanoporous Membranes

Type	Thickness	Precision	Diameter
Ceramic Membrane	2 mm	10 μm	50 mm
Titanium Membrane	2 mm	20 μm	50mm

The physical images of the membrane samples used in the experiment are shown in Figure 1.



Figure 1. Physical Image of the Membrane Sample

2.2 Experimental Principles and Methods

In engineering applications, porous structures often exhibit complex pore distributions and geometries, making precise modeling challenging. To simplify calculations, it is common to introduce a momentum source term that is related to the flow velocity to approximate the flow characteristics

in these regions. This method avoids detailed modeling of complex geometries, and its fundamental principle is to effectively describe the flow resistance of fluid in porous media by adding an additional resistance source term in the fluid dynamics equations^[8]. The expression for this source term is:

$$S_i = - \left(\sum_{j=1}^3 D_{ij} \mu v_j \sum_{j=1}^3 C_{ij} \frac{1}{2} \rho |v| v_j \right) \quad (1)$$

In the equation, S_i represents the momentum source term in the $i(x,y,z)$ direction, v is the velocity, D and C are specified matrices, μ is the dynamic viscosity of the gas, and ρ is the gas density. The first term represents the viscous loss, while the second term represents the inertial loss. For porous media, this can be rewritten as:

$$S_i = - \left(\frac{\mu}{\alpha} v_i + \frac{1}{2} C_2 \rho |v| v_i \right) \quad (2)$$

In the equation, α represents the permeability, C_2 is the inertial resistance coefficient, and at this point, the matrix D is denoted as $\frac{1}{\alpha}$. The momentum sink term generates a pressure gradient in the fluid, denoted as $\nabla p = S_i$, which corresponds to $\nabla p = S_i \Delta n$, with Δn being the thickness of the porous medium. Therefore, the porous media model can be expressed by the following equation:

$$S_i = \left(\frac{\mu}{\alpha} v + \frac{1}{2} C_2 \rho v^2 \right) \Delta n \quad (3)$$

By fitting the relationship between the pressure field and the velocity field in the experimental setup, the following expression can be obtained:

$$\Delta p = av^2 + bv \quad (4)$$

Therefore, the viscous resistance coefficient and the inertial resistance coefficient of the porous medium are:

$$\frac{1}{\alpha} = \frac{b}{\mu \Delta n} \quad (5)$$

$$C_2 = \frac{2a}{\rho \Delta n} \quad (6)$$

2.3 Experimental Equipment Design

In this experiment, the gas is pressurized by a pump, then passes through a rectifier before entering the experimental pipeline. It flows sequentially through a high-pressure detection point, the porous media region, a low-pressure detection point, and an anemometer. Data from the high and low-pressure detection points and the anemometer can be used to quantitatively analyze the fluid resistance of the porous media^[9]. The schematic and physical images of the porous media resistance measurement equipment are shown in Figures 2 and 3. The main components include a pressure transmitter (1), bracket (2), exhaust pipe (3), flange (4), porous media (5), intake pipe (6), airflow stabilizer (7), and intake interface (8).

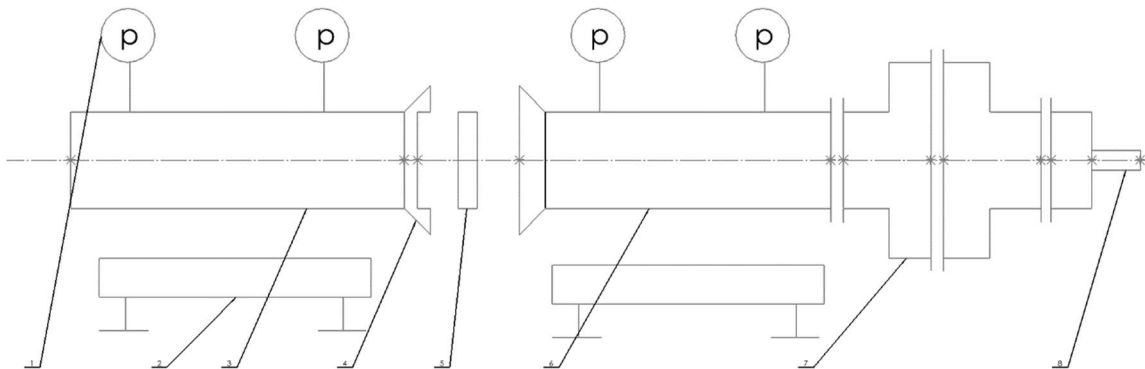


Figure 2. Porous media resistance coefficient measurement equipment structure diagram



Figure 3. Physical Image of Porous Media Resistance Coefficient Measurement Equipment

3. Data Collection and Processing

Data collection is accomplished through a data acquisition system installed on the experimental setup. The system consists of several key components, including a Programmable Logic Controller (PLC), a touchscreen, communication cables, and multiple pressure sensors. The Modbus signal sensors are connected to the PLC via RS485 communication cables for real-time data transmission and monitoring. During the experiment, the gas flows sequentially through the high-pressure and low-pressure monitoring points, recording the pressure changes before and after passing through the porous media. By measuring the pressure differential, the pressure drop as the gas flows through the porous media can be accurately obtained. Meanwhile, the anemometer continuously monitors the gas velocity as it passes through the porous media. Table 2 shows the measured pressure drop and corresponding velocity data for porous media materials, including ceramic membranes and titanium membranes.

Table 2. Flow Velocity and Pressure Drop of Porous Membranes

Porous Media Material	Serial No.	Experiment Temperature (°C)	Wind Speed (m/s)	Pressure Drop (Pa)
Ceramic Membrane	1	28	5.6	20000
	2	28	5.0	18500
	3	28	4.6	17500
	4	28	4.4	16500
	5	28	4.1	14500
Titanium Membrane_1	1	28	3.8	30500
	2	28	3.5	27000
	3	28	3.1	22500
	4	28	2.6	18000
	5	28	1.5	8750
Titanium Membrane_2	1	28	4.0	22000
	2	28	3.4	19000
	3	28	2	9000
	4	28	1.8	8000
	5	28	1.65	6750

Based on the formulas for the viscous resistance coefficient and inertial resistance coefficient of porous media in Section 2.2, the relationship between pressure drop and flow velocity during the fluid passage through the porous media can be obtained from experimental data. To further determine the viscous and inertial resistance coefficients, it is necessary to perform mathematical modeling of the pressure drop and flow velocity relationship. By fitting the experimental data of pressure drop and flow velocity, the correlation coefficients for viscous and inertial resistance can be solved.

In this study, the curve_fit function provided by the scipy.optimize module in Python programming language is used to perform curve fitting. curve_fit is a nonlinear least squares fitting tool^[10], which works by minimizing the differences between experimental data and the fitting function to solve the unknown parameters in the function. The method is based on least squares, where it minimizes the squared error between experimental data points and the fitted curve to determine the optimal parameters. Specifically, it iterates in parameter space to find the parameter combination that minimizes the error function. The following Figures 4 to 6 show the pressure drop and flow velocity fitting curves for ceramic membrane, titanium membrane_1, and titanium membrane_2, respectively.

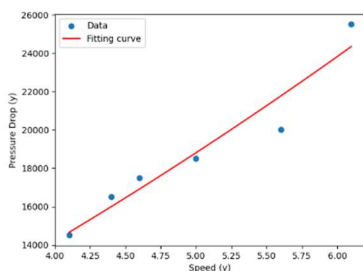


Figure 4. Pressure Drop vs. Flow Velocity Curve for Ceramic Membrane

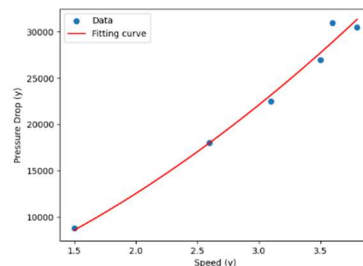


Figure 5. Pressure Drop vs. Flow Velocity Curve for Titanium Membrane_1

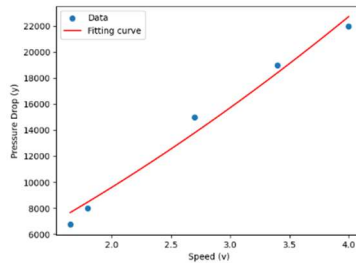


Figure 6. Pressure Drop vs. Flow Velocity Curve for Titanium Membrane_1

From the above fitting curves, it can be observed that the fitted curves match well with the experimental data points, indicating a good fitting performance. Here, the concept of the goodness of fit (R^2), also known as the coefficient of determination, R^2 is introduced as a key metric for evaluating the effectiveness of the regression model. It represents the proportion of variance in the data explained by the model. Specifically, it reflects the extent to which flow velocity explains the pressure drop. The R^2 is expressed by Equation 7.

$$R^2 = 1 - \frac{\sum (y_{tru} - y_{pred})^2}{\sum (y_{tru} - \bar{y})^2} \quad (7)$$

In this equation:

y_{tru} represents the experimental values,

y_{pred} denotes the predicted values obtained from the fitting model,

\bar{y} is the mean of y_{pred} .

The coefficient of determination R^2 ranges between 0 and 1. The closer it is to 1, the better the curve fitting performance. In this study, the R^2 values of the fitted curves are all greater than 0.9, indicating a strong agreement with the experimental data. Table 3 presents the coefficients of the fitted curves and their corresponding R^2 values:

Table 3. Basic Parameters of Micro/Nanoporous Membranes

Porous Membrane Type	Mathematical Expression	R^2
Ceramic Membrane	$\Delta p = 208.9v^2 + 2716.7v$	0.928
Titanium Membrane_1	$\Delta p = 1109.1v^2 + 4036.8v$	0.983
Titanium Membrane_2	$\Delta p = 440.7v^2 + 3917.4v$	0.983

During the experiment, the test gas used was air, with a density of 1.225 kg/m^3 and a dynamic viscosity of $1.7894 \times 10^{-5} \text{ Pa}\cdot\text{s}$. Based on Table 3 and formulas (5) and (6), the viscous resistance coefficient and inertial resistance coefficient for each type of membrane can be determined. Table 4 presents the calculated resistance coefficients.

Table 4. Porous Membrane Resistance Coefficients

Porous Membrane Type	Viscous Resistance Coefficient / $Pa \cdot s \cdot m^{-2}$	Inertial Resistance Coefficient / $Pa \cdot s^2 \cdot m^{-4}$
Ceramic Membrane	$7.50 \cdot 10^{10}$	$1.70 \cdot 10^5$
Titanium Membrane_1	$1.12 \cdot 10^{10}$	$9.05 \cdot 10^5$
Titanium Membrane_2	$1.08 \cdot 10^{11}$	$3.60 \cdot 10^5$

Based on the obtained viscous resistance coefficient and inertial resistance coefficient, the experiment was simulated using Ansys Fluent 2022 R1 for validation. By replicating the experimental environment in the simulation, the pressure drop before and after the micro-nano porous membrane was numerically simulated, and the error between the simulation results and the experimental data was evaluated^[11]. The mesh generation results of the experimental pipeline are shown in Figure 7.

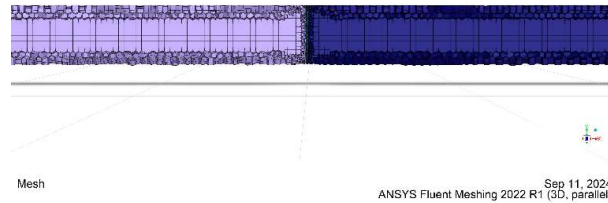


Figure 7. The mesh diagram of the experimental pipe section.

Table 5. Simulated pressure drop error table

Porous Media Material	Pressure Drop (Pa)		Error(%)
	Experimental Data	Numerical Simulation	
Ceramic Membrane	20000	21131	5.6
	18500	18258	1.3
	17500	16424	6.1
	16500	15533	5.8
Titanium Membrane_1	14500	14225	1.8
	30500	30528	0.09
	27000	26987	0.04
	22500	22568	0.2
Titanium Membrane_2	18000	17527	2.6
	8750	8333	4.7
	22000	22059	0.2
	19000	17878	5.9
	9000	9314	3.4
	8000	8226	2.8
	6750	6559	2.8

The experimental model includes three fluid domains: the high-pressure zone, the intermediate porous medium zone, and the low-pressure zone. Since the fluid flow in the porous medium zone is approximately laminar, the laminar flow model is used in the simulation, with a pressure-based steady-state solver and the SIMPLE method to iteratively correct the pressure and velocity fields, improving convergence speed. Air is considered incompressible at low speeds. To verify the accuracy of the model, the average pressure difference across the high and low-pressure zone measurement points is compared with the experimental pressure drop. The analysis of the simulated data shows that the maximum error in pressure drop is 5.9%, and the minimum error is 0.04%, confirming the reasonableness and accuracy of the measured viscous and inertial resistance coefficients. The errors may arise from factors such as grid resolution and the chosen solution method. The simulation error table is shown in Table 5.

4. Conclusion

Based on the porous media viscous resistance experimental platform, the viscous resistance coefficient and inertial resistance coefficient of foam titanium membranes and ceramic membranes were precisely determined through polynomial fitting of the velocity-pressure drop curve. Computational Fluid Dynamics (CFD) simulations were employed to validate the calculated results, showing that the pressure drop simulation error ranged from 0.04% to 5.9%. Compared to the pressure drop simulation errors reported by Ding et al^[11], the errors in this study were significantly lower. This demonstrates the high accuracy and strong practicality of the proposed method, providing an effective technical approach for measuring the resistance coefficients of microporous membranes.

References

- [1] ARUMUGHAM T, KALEEKKAL N J, GOPAL S, et al. Recent developments in porous ceramic membranes for wastewater treatment and desalination: A review [J]. *Journal of Environmental Management*, 2021, 293: 112925.
- [2] ZHAO M, LIU Y, ZHANG J, et al. Janus ceramic membranes with asymmetric wettability for high-efficient microbubble aeration [J]. *Journal of Membrane Science*, 2023, 671: 121418.
- [3] Wenming Fa. Study on the Treatment of Domestic Sewage by Micro-Nano Aeration and Membrane-Fixed Artificial Wetlands [J]. *Advances in Environmental Protection*, 2021, 11: 958.
- [4] Wu Guozhong, Xing Yongqiang, Lv Yan, et al. Experimental Analysis of Flow Resistance Coefficients of Oil-Water in Porous Media [J]. *Experimental Technology and Management*, 2016, 33(10): 34-37.
- [5] Xin Li, Hu Xingjun, Hui Zheng, et al. Measurement Method and Device for Viscous Resistance Coefficient and Inertial Resistance Coefficient of Porous Media, CN106706268A [P/OL].
- [6] AL SHAMI E, WANG Z, WANG X. Non-linear dynamic simulations of two-body wave energy converters via identification of viscous drag coefficients of different shapes of the submerged body based on numerical wave tank CFD simulation [J]. *Renewable Energy*, 2021, 179: 983-997.
- [7] SIMAVILLA D N, ELLERO M. Mesoscopic simulations of inertial drag enhancement and polymer migration in viscoelastic solutions flowing around a confined array of cylinders [J]. *Journal of Non-Newtonian Fluid Mechanics*, 2022, 305: 104811.
- [8] Liu Dongdong, Li Xingping, Li Yue, et al. Calculation Method and Device for the Performance of a Sand Prevention Device, CN115828671A [P/OL].
- [9] Huang Zundi, Liang Xifeng, Chang Ning. Experimental Study on the Resistance Coefficient of Porous Plates in a Vacuum Chamber [J]. *Journal of Engineering Thermophysics*, 2018, 39(12): 2657-2664.
- [10] Wei Heyu, Xu Jian. Downhill Coasting and Regenerative Braking Method for Autonomous Vehicles Based on Piecewise Least Squares Fitting [J]. *Hydraulic Pneumatics and Sealing*, 2025, 45(02): 79-85.
- [11] Ding Wensi, Zhang Haida. Device and Method for Measuring Viscous Resistance Coefficient and Inertial Resistance Coefficient of Porous Media, CN117705669A [P/OL].